Prospects of Indirect Detection for the Heavy S3 Dark Doublet*

Catalina Espinoza

Instituto de Física, UNAM

*C.E. and M. Mondragón, e-Print:2008.11792 [hep-ph]

Outline

Introduction

Dark Matter

In the particle dark matter (DM) hypothesis, dark matter is composed of elementary particles

- They only interact through the gravitational force (we know this)
- Hopefully(!) also through another force, very weakly though
- Their annihilation can produce known particles that can be detected

They can be detected indirectly from their annihilation products!

Gamma rays from DM

In particular, annihilation of DM particles can produce gamma rays.

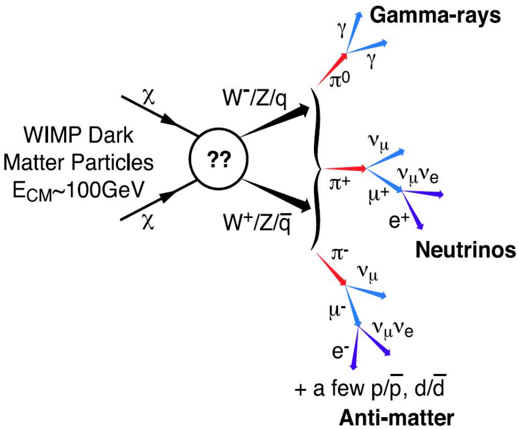

Products of annihilation processes.

What is Indirect Detection of DM?

In this manner, detection of annihilation products like gamma rays or other particles constitutes an indirect way to pinpoint DM

Observing the sky can shed light on the nature of DM

Observing gamma rays

We will focus here on gamma ray observatories, in particular the Cherenkov Telescope Array

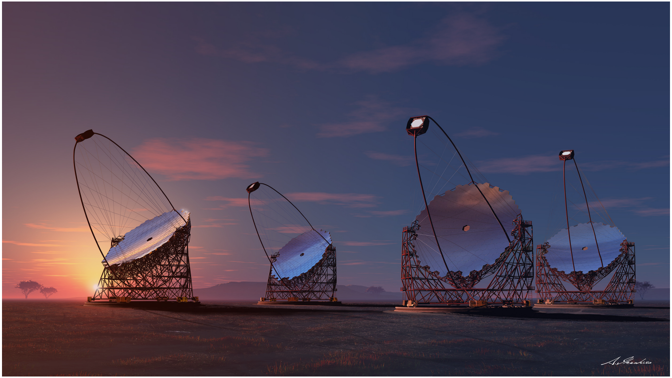

Artist conception of the CTA

Observing gamma rays

From the CTA website

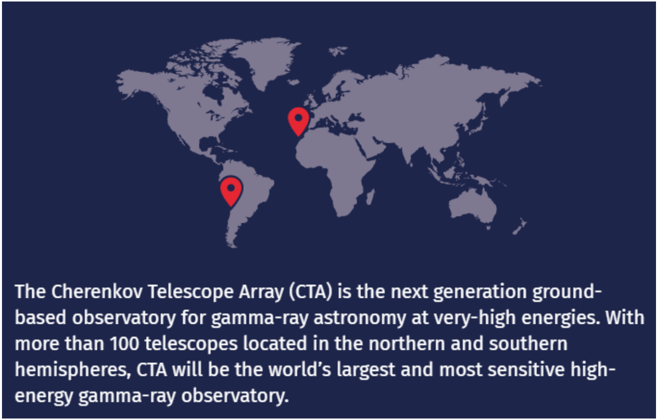

Construction was expected to begin in 2020

Gamma rays from DM

But did the gamma rays observed originated from DM? How can we tell?

- Regions of high DM density are selected for observation
- Known sources of gamma rays (e.g. Gamma Ray Bursts (GRB) etc) are treated as background
- Any signal above background could potentially be attributed to DM annihilation

Dwarf galaxies are very attractive $\rightarrow$ low backgrounds

The Dark S3 Doublet

The Dark S3 Doublet

This model features an S3 symmetric extension of the scalar sector of the Standard Model (SM) including a scalar $SU(2)$ doublet dark matter candidate.

- We accommodate two $SU(2)$ electroweak doubles in an $S3$ doublet:

$$\begin{pmatrix} \Phi_1 \\ \Phi_2 \end{pmatrix} \sim 2 \tag{1}$$

- And two $SU(2)$ electroweak doubles transforming as the symmetric and anti-symmetric singlet representations of $S3$:

$$\Phi_S \sim 1_S \ , \ \Phi_a \sim 1_A \tag{2}$$

The Scalar Potential

The scalar potential becomes fairly complicated:

$$V = V_2 + V_4 + V_{4s} + V_{4a} + V_{4sa}, \tag{3}$$

V_2 comprises the quadratic terms:

$$V_2 = \mu_0^2 \Phi_s^\dagger \Phi_s + \mu_1^2 (\Phi_1^\dagger \Phi_1 + \Phi_2^\dagger \Phi_2) + \mu_2^2 \Phi_a^\dagger \Phi_a, \tag{4}$$

while V_4 contains quartic terms involving Φ_1 and Φ_2 only:

$$\begin{aligned} V_4 &= \lambda_1 (\Phi_1^\dagger \Phi_1 + \Phi_2^\dagger \Phi_2)^2 + \lambda_2 (\Phi_1^\dagger \Phi_2 - \Phi_2^\dagger \Phi_1)^2 \\ &\quad + \lambda_3 [(\Phi_1^\dagger \Phi_1 - \Phi_2^\dagger \Phi_2)^2 + (\Phi_1^\dagger \Phi_2 + \Phi_2^\dagger \Phi_1)^2], \end{aligned} \tag{5}$$

The Scalar Potential is S3-Symmetric

while V_{4s} and V_{4a} represent the quartic terms involving Φ_s and Φ_a respectively:

$$\begin{aligned} V_{4s} \;=\; & \lambda_4[(\Phi_s^\dagger\Phi_1)(\Phi_1^\dagger\Phi_2+\Phi_2^\dagger\Phi_1)+(\Phi_s^\dagger\Phi_2)(\Phi_1^\dagger\Phi_1-\Phi_2^\dagger\Phi_2)+\mathrm{h.c.}] \\ & +\lambda_5(\Phi_s^\dagger\Phi_s)(\Phi_1^\dagger\Phi_1+\Phi_2^\dagger\Phi_2) \\ & +\lambda_6[(\Phi_s^\dagger\Phi_1)(\Phi_1^\dagger\Phi_s)+(\Phi_s^\dagger\Phi_2)(\Phi_2^\dagger\Phi_s)] \\ & +\lambda_7[(\Phi_s^\dagger\Phi_1)(\Phi_s^\dagger\Phi_1)+(\Phi_s^\dagger\Phi_2)(\Phi_s^\dagger\Phi_2)+\mathrm{h.c.}] \\ & +\lambda_8(\Phi_s^\dagger\Phi_s)^2 \end{aligned} \tag{6}$$

The expression for V_{4a} is very similar to eq. (6) with Φ_a replacing Φ_s and quartic couplings $\lambda_9, \ldots, \lambda_{13}$, except that the λ_9 term analogous to the λ_4 term has Φ_1 and Φ_2 interchanged.

Z_2 symmetry to ensure an stable DM candidate

Finally the mixed Φ_s, Φ_a term is given by:

$$V_{4sa} = \lambda_{14}(\Phi_s^\dagger \Phi_a \Phi_a^\dagger \Phi_s) + \lambda_{15}(\Phi_1^\dagger \Phi_s \Phi_2^\dagger \Phi_a + \mathrm{h.c.}) \tag{7}$$

We choose Φ_a as the dark doublet, comprising three dark scalars. In order to force the scalar DM candidate to be stable we introduce an additional discrete Z_2 symmetry with respect to which all fields are even except those with subindex a, taken as Z_2-odd. This gets rid of the λ_9 and λ_{15} term in the potential leaving only terms with even powers of Φ_a.

Vacuum Expectation Values

After electroweak symmetry breaking all the scalar doublets acquire a vacuum expectation value (vev) denoted by v_s, v_1, v_2 and v_a respectively. However, in order to avoid the explicit breaking of the Z_2 symmetry we fix $v_a = 0$. Consistency of the minimization (tadpole) equations

$$\partial V/\partial v_i = 0 \tag{8}$$

requires the alignment of 2 vevs:

$$v_1 = \sqrt{3} v_2, \tag{9}$$

with the usual SM vev given by $v = \sqrt{v_s^2 + 4v_2^2} = 246\,\mathrm{GeV}$.

EWSM mixing

We choose $\tan\theta = 2v_2/v_s$ as one of the independent parameters in the numerical calculations and parametrize the Higgs doublets as

$$\Phi_s = \begin{pmatrix} h_s'^{+} \\ (v_s + h_s'^{n} + i h_s'^{p})/\sqrt{2} \end{pmatrix} \tag{10}$$

and similarly for Φ_1, Φ_2 and Φ_a. EWSB induces mixing between the Z_2 even scalars while the Z_2 odd fields do not mix, and therefore the mass and mixing matrices have block diagonal form.

Mixing matrices

In the case of the neutral scalar fields the submatrix mixing the Z_2 even fields $h_s'^n$, $h_1'^n$ and $h_2'^n$ into the mass eigenstates H, H_3 and h takes the form:

$$Z^h = \begin{pmatrix} \cos(\alpha) & 0 & \sin(\alpha) \\ 0 & 1 & 0 \\ -\sin(\alpha) & 0 & \cos(\alpha) \end{pmatrix} \begin{pmatrix} 1 & 0 & 0 \\ 0 & \frac{1}{2} & -\frac{\sqrt{3}}{2} \\ 0 & \frac{\sqrt{3}}{2} & \frac{1}{2} \end{pmatrix} \tag{11}$$

The rotation angle α is a complicated function of the parameters (quartic couplings etc.)

Mixing matrices

The charged and CP-odd scalars mix with the matrix:

$$Z^C = Z^A = \begin{pmatrix} \cos(\theta)\sin(\theta) & 0 & \sin^2(\theta) \\ 0 & 1 & 0 \\ -\cos(\theta)\sin(\theta) & 0 & \cos^2(\theta) \end{pmatrix} \begin{pmatrix} 1 & 0 & 0 \\ 0 & \frac{1}{2} & -\frac{\sqrt{3}}{2} \\ 0 & \frac{\sqrt{3}}{2} & \frac{1}{2} \end{pmatrix} \tag{12}$$

The decoupling limit

The connection of H and h with the SM Higgs is done as usual through the decoupling limit defined by the relation

$$\cos(\theta - \alpha) \approx 0 \tag{13}$$

in this limit h has SM-like couplings and can be identified with the SM Higgs. There are 15 free parameters of the model: λ_1 - λ_8, λ_{10} - λ_{14}, $\tan\theta$ and μ_2 but one is eliminated by fixing the mass of h to the SM Higgs mass.

The physical scalars

There are 10 physical scalars in the model, we use interchangeably the following two notations, $\tilde{h}_k$ with $k = 1, 2, 3$ for the neutral scalars H, H_3 and h, i.e.

$$\tilde{h}_1 = H, \tilde{h}_2 = H_3 \text{ and } \tilde{h}_3 = h, \tag{14}$$

$\tilde{A}_k$ for the neutral pseudo-scalars G^0, A_3 and A, and $\tilde{H}_k^{\pm}$ for the charged scalars $G^{\pm}$, $H_3^{\pm}$ and $H^{\pm}$, and in the dark sector we have the fields h_a, A_a and $H_a^{\pm}$ with h_a the DM candidate.

It is favorable to work with the set of physical masses of the scalars as independent variables alongside with the parameters μ_2, λ_{13}, λ_{14}, $\tan\theta$ and α, so we invert the expressions for the masses obtaining...

The masses as independent parameters

$$
\begin{aligned}
\lambda_1 &= \left(\csc^2\theta(9\cos(2\alpha)(M_h^2 - M_H^2) + 9M_h^2 + 9M_H^2 + 18M_{H_3^\pm}^2 - 2M_{H_3}^2 - 18M_{H^\pm}^2) + 18M_{H^\pm}^2\right)/(36v^2) \\
\lambda_2 &= \left(\csc^2\theta(-M_{A_3}^2 + M_{H_3^\pm}^2 + M_A^2 - M_{H^\pm}^2) - M_A^2 + M_{H^\pm}^2\right)/(2v^2) \\
\lambda_3 &= \csc^2\theta(9M_{H^\pm}^2\cos(2\theta) - 18M_{H_3^\pm}^2 + 8M_{H_3}^2 + 9M_{H^\pm}^2)/(36v^2) \\
\lambda_4 &= -2M_{H_3}^2\csc\theta\sec\theta/(9v^2) \\
\lambda_5 &= \left(9\sin(2\alpha)\csc\theta\sec\theta(M_H^2 - M_h^2) + 2M_{H_3}^2\sec^2\theta + 36M_{H^\pm}^2\right)/(18v^2) \\
\lambda_6 &= \left(M_{H_3}^2\sec^2\theta + 9M_A^2 - 18M_{H^\pm}^2\right)/(9v^2) \\
\lambda_7 &= \left(M_{H_3}^2\sec^2\theta - 9M_A^2\right)/(18v^2) \\
\lambda_8 &= \sec^2\theta\left(9\cos(2\alpha)(M_H^2 - M_h^2) - 2M_{H_3}^2\tan^2(\theta) + 9(M_h^2 + M_H^2)\right)/(36v^2) \\
\lambda_{10} &= 2(M_{H_a^\pm}^2 - \mu_2^2)\csc^2\theta/v^2 \\
\lambda_{11} &= -\left(\lambda_{14}v^2\cot\theta^2 - M_{h_a}^2\csc^2\theta - M_{A_a}^2\csc^2\theta + 2M_{H_a^\pm}^2\csc^2\theta\right)/v^2 \\
\lambda_{12} &= \left(\csc^2\theta(M_{h_a}^2 - M_{A_a}^2)\right)/(2v^2)
\end{aligned}
\tag{15}
$$

These expressions are useful because in the directed scan it is simpler to vary the masses to probe the regions we are interested the most.

Enhanced annihilating cross section

In the large DM mass regime it is important to take into account the nonperturbative phenomenon of Sommerfeld enhancement

- This phenomenon occurs because the DM particles move at present with nonrelativistic (NR) velocities ($\sim 10^{-3}$) and have enough time to exchange (on-shell) mediators before the actual annihilation.
- For large DM masses, the electroweak force between the DM pair then becomes "long range".
- The EWSB induced mass splitting between the heavy DM particles in the same $SU(2)$ multiplet is small and as a result the exchange of mediators can induce transitions of the original annihilating DM pair to other states in the multiplet.

Enhanced annihilating cross section

- As a result, the wave function of the DM pair is no longer a plane wave and to correctly predict the annihilation cross section it is necessary to find out the modified wave function.
- The dominant contributions of higher order are the ladder type diagrams where multiple exchanges of on-shell mediators take place before the actual annihilation of the DM pairs.
- For the numerical scan we will assume the DM sector quasi-degenerate in mass $M_{h_a} \simeq M_{A_a} \simeq M_{H_a^\pm}$.

Exchange diagrams

Schematically ...

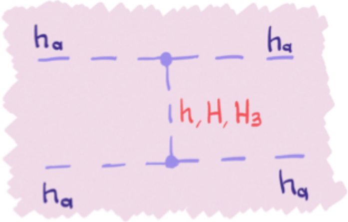

Exchange diagram $h_a h_a \to h_a h_a$

From the tree level allowed diagrams for the process $h_a h_a \to h_a h_a$ ...

Ladder diagrams

The multiple exchange is described by ladder diagrams

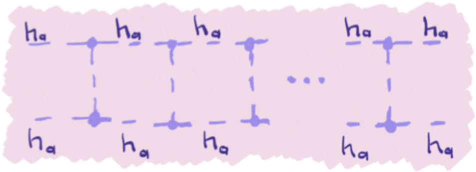

Ladder diagram with multiple exchanges

Ladder diagrams

When the mass splitting between the DM particles is small, the kinematical window opens for the rest of the allowed processes

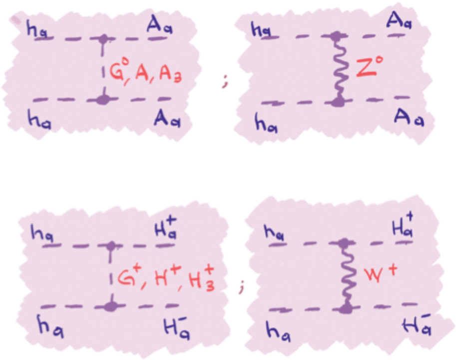

Exchange diagrams $h_a h_a \rightarrow$ DM DM

Matrix Potential

In turn, these allow for the complete exchange diagrams, i.e. all the possible scattering amplitudes can ocurr internally in the ladder: $h_a h_a \to \mathrm{DMDM}$, $A_a A_a \to \mathrm{DMDM}$ and $H_a^+ H_a^- \to \mathrm{DMDM}$ where DMDM here means either of $h_a h_a$, $A_a A_a$ or $H_a^+ H_a^-$.

- The ladder diagrams cannot be solved in the full theory.
- Luckily, the processes are not relativistic.
- It is sufficient to find out the effective NR potentials induced by the exchange of the different gauge bosons and scalars.
- We end up with a matrix whose elements are the NR potentials, the matrix is constructed in the basis of 2-particle states $\{h_a h_a, A_a A_a, H_a^+ H_a^-\}$

Matrix Potential

For instance:

$$V_{11}(r) = \frac{1}{4M_{h_a}^2} \int \frac{d^3q}{(2\pi)^3} e^{i\mathbf{q}\cdot\mathbf{r}} iA_{\rm NR}^{\rm 2\text{-}body}(h_a h_a \to h_a h_a) \qquad (16)$$

where r is the relative coordinate of the two-particle state. The subindex in the potential refers to the basis of 2-particle states $\{h_a h_a, A_a A_a, H_a^+ H_a^-\}$. In this manner we obtain for the potential matrix:

$$V(r) = V_1(r) + V_2(r) \qquad (17)$$

Matrix Potential

The first term corresponds to the exchange of scalar mediators:

$$V_1(r) = \begin{pmatrix} \frac{-|s^{h_a h_a}_{\tilde{h}_k}|^2 e^{-M_{\tilde{h}_k} r}}{16\pi M^2_{h_a} r} & \frac{-|s^{h_a A_a}_{\tilde{A}_k}|^2 e^{-M_{\tilde{A}_k} r}}{16\pi M^2_{h_a} r} & \frac{-|s^{h_a H^\pm_a}_{\tilde{H}^\pm_k}|^2 e^{-M_{\tilde{H}^\pm_k} r}}{16\pi M^2_{h_a} r} \\ \frac{-|s^{h_a A_a}_{\tilde{A}_k}|^2 e^{-M_{\tilde{A}_k} r}}{16\pi M^2_{h_a} r} & \frac{-|s^{A_a A_a}_{\tilde{h}_k}|^2 e^{-M_{\tilde{h}_k} r}}{16\pi M^2_{h_a} r} + 2(M_{A_a} - M_{h_a}) & \frac{-|s^{A_a H^\pm_a}_{\tilde{H}^\pm_k}|^2 e^{-M_{\tilde{H}^\pm_k} r}}{16\pi M^2_{h_a} r} \\ \frac{-|s^{h_a H^\pm_a}_{\tilde{H}^\pm_k}|^2 e^{-M_{\tilde{H}^\pm_k} r}}{16\pi M^2_{h_a} r} & \frac{-|s^{A_a H^\pm_a}_{\tilde{H}^\pm_k}|^2 e^{-M_{\tilde{H}^\pm_k} r}}{16\pi M^2_{h_a} r} & \frac{-|s^{H^\pm_a H^\pm_a}_{\tilde{h}_k}|^2 e^{-M_{\tilde{h}_k} r}}{16\pi M^2_{h_a} r} + 2(M_{H^\pm_a} - M_{h_a}) \end{pmatrix} \tag{18}$$

with implicit sums over k. It is customary to include the mass spliting terms in the diagonal which are generated by perturbative higher order terms due to EWSB.

Matrix Potential

The second term corresponds to the exchange of gauge boson mediators:

$$V_2(r) = \begin{pmatrix} 0 & -\frac{g_2^2 e^{-M_Z r}}{16\pi c_w^2 r} & -\frac{g_2^2 e^{-M_W r}}{16\pi r} \\ -\frac{g_2^2 e^{-M_Z r}}{16\pi c_w^2 r} & 0 & -\frac{g_2^2 e^{-M_W r}}{16\pi r} \\ -\frac{g_2^2 e^{-M_W r}}{16\pi r} & -\frac{g_2^2 e^{-M_W r}}{16\pi r} & -\frac{g_2^2 (s_w^2 + (1-2s_w^2)^2 e^{-M_Z r})}{16\pi c_w^2 r} \end{pmatrix} \tag{19}$$

Here g_2 is the weak coupling constant, $s_w = \sin\theta_w$, $c_w = \cos\theta_w$ with θ_w the Weinberg angle.

Couplings

The couplings are of the form:

$$
\begin{aligned}
s_{\tilde{h}_k}^{h_a h_a} &= -i[v\sin\theta(\lambda_{10}+\lambda_{11}+\lambda_{12})(\sqrt{3}Z^h_{k2}+Z^h_{k3})/2 + v\cos\theta\lambda_{14}Z^h_{k1}] \\
s_{\tilde{h}_k}^{A_a A_a} &= -i[v\sin\theta(\lambda_{10}+\lambda_{11}-2\lambda_{12})(\sqrt{3}Z^h_{k2}+Z^h_{k3})/2 + v\cos\theta\lambda_{14}Z^h_{k1}] \\
s_{\tilde{h}_k}^{H_a^\pm H_a^\pm} &= -i\lambda_{10}v\sin\theta(\sqrt{3}Z^h_{k2}+Z^h_{k3})/2 \\
s_{\tilde{A}_k}^{h_a A_a} &= -2i\lambda_{12}v\sin\theta(\sqrt{3}Z^A_{k2}+Z^A_{k3})/2 \\
s_{\tilde{H}_k^\pm}^{h_a H_a^\pm} &= (-i/2)[\lambda_{14}v\cos\theta Z^C_{k1} + v\sin\theta(2\lambda_{12}+\lambda_{11})(\sqrt{3}Z^C_{k2}+Z^C_{k3})/2] \\
s_{\tilde{H}_k^\pm}^{A_a H_a^\pm} &= (-i/2)[\lambda_{14}v\cos\theta Z^C_{k1} + v\sin\theta(-2\lambda_{12}+\lambda_{11})(\sqrt{3}Z^C_{k2}+Z^C_{k3})/2]
\end{aligned}
\tag{20}
$$

Deformed Wave Function

The deformed wave function is obtained by solving (numerically) a Schrödinger like system of equations:

$$h'(r) + h^2(r) + \frac{1}{4} M_{h_a}^2 v_{\rm rel}^2 - M_{h_a} V(r) = 0 \qquad (21)$$

with the matrix $h(r)$ satisfying the boundary condition

$$h(\infty) = (iM_{h_a} v_{\rm rel}/2)\sqrt{1 - 4V(\infty)/(M_{h_a} v_{\rm rel}^2)} \qquad (22)$$

where $v_{\rm rel} \sim 2 \times 10^3$ is the present day relative velocity of annihilating DM.

Sommerfeld Factors

Having found the solution for the matrix $h(r)$, the column vector defined as

$$d \equiv (d_{11}\ d_{12}\ d_{13})^T \tag{23}$$

contains the Sommerfeld factors which are calculated from the relation:

$$dd^\dagger = \frac{1}{iM_{h_a} v_{\mathrm{rel}}}(h(0) - h^\dagger(0)) \tag{24}$$

the matrix $dd^\dagger$ has only one nonzero eigenvalue corresponding to its eigenvector d, note that this eigenvalue is just the modulus square of d.

Sommerfeld Factors

In this figure we show the variation of the Sommerfeld factors with the DM mass, other free parameters are taken as in the benchmark or Best Fit Point (BFP) shown later.

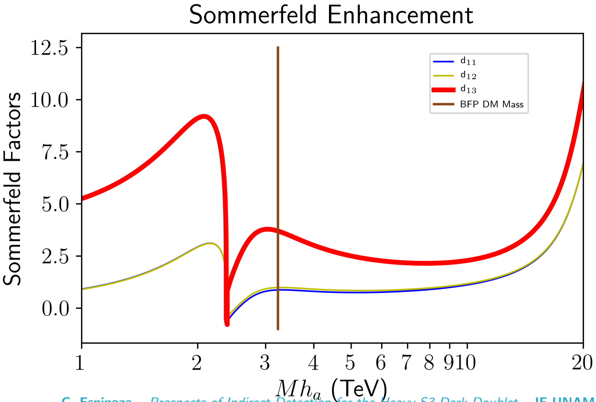

Sommerfeld Factors

- We note that the three factors become slightly negative and close to zero around a DM mass of $\sim$ 2.3 TeV
- This suggests that around these values of parameter space a marked destructive interference is at work
- The BFP does not occurs in the vicinity of the highest enhancements and thus other important physical constraints weight in to shift it to a higher mass

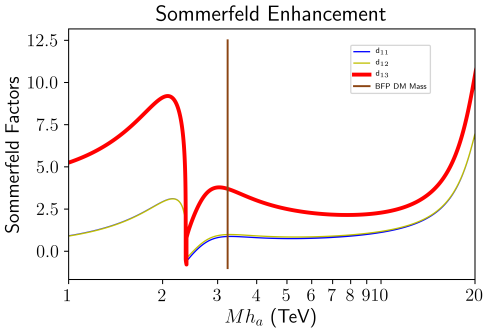

Annihilation Cross Sections

The annihilating cross section in the limit of zero relative velocity for a given final state f is then given by:

$$\sigma v_{\mathrm{rel}}(h_a\, h_a \to f) = \frac{1}{2}(D\Gamma^f D^\dagger)_{11} \tag{25}$$

where

$$\Gamma = \sum_f \Gamma^f \tag{26}$$

is the total matrix of absorptive terms to all final states f, and D is the matrix whose only nonzero row (in our basis the first row) is d^{T}.

Absorptive Matrices

The elements of Γ^f are given explicitly by

$$\Gamma^f_{ij} = \frac{N_i N_j}{4M^2_{h_a}} \int \prod_{a\in f} \frac{d^3 q_a}{(2\pi)^3 2E_a} \mathcal{M}(i \to f)\mathcal{M}^*(j \to f)(2\pi)^4 \delta^4(p_i - p_j) \tag{27}$$

here the indexes i and j refer to any element of the two-particle basis (the annihilating pair), f is any allowed final state of non-DM particles in the model, p_i and p_j are the 4-momenta of the initial and final states and the symmetry factors are given by $N_{h_a h_a} = N_{A_a A_a} = 1/\sqrt{2}$ and $N_{H_a^+ H_a^-} = 1$, with $\mathcal{M}$ the tree level corresponding annihilating amplitudes.

Absorptive Matrices

We compute Γ^f for the following final states: $\gamma\gamma$, γZ, ZZ, W^+W^-, HH, H_3H_3, hh and Hh (for HH_3 and H_3h, Γ^f is zero). For example, $\Gamma^{H_3H_3}$ is given by:

$$\Gamma^{H_3H_3} = \frac{1}{32\pi M_{h_a}^2}\begin{pmatrix} \frac{1}{2}\lambda_+^2 & \frac{9}{2}\lambda_-\lambda_+ & \frac{9}{\sqrt{2}}\lambda_{10}\lambda_+ \\ \frac{9}{2}\lambda_-\lambda_+ & \frac{1}{2}\lambda_-^2 & \frac{9}{\sqrt{2}}\lambda_{10}\lambda_- \\ \frac{9}{\sqrt{2}}\lambda_{10}\lambda_+ & \frac{9}{\sqrt{2}}\lambda_{10}\lambda_- & \lambda_{10}^2 \end{pmatrix} \tag{28}$$

where $\lambda_\pm \equiv \lambda_{10} + \lambda_{11} \pm 2\lambda_{12}$. Note that for this calculations we approximate the DM mass splittings as zero and we also neglect terms of the form M_X/M_{h_a} with X any gauge boson or scalar, for the numerical calculation we thus will keep the masses of the scalars to relatively light values.

Gamma Ray Yields

The total differential cross section into gammas is given by

$$\frac{d\sigma v_{\rm rel}}{dE_\gamma} = \sum_f \sigma v_{\rm rel}(h_a h_a \to f) \times \frac{dN^f}{dE\gamma} \tag{29}$$

For the case of continuous yields (f = EW or scalar boson pair as final state) we use the parametrization (Astropart. Phys. 9 (1998), pp. 137–162, arXiv: astro-ph/9712318 [astro-ph]):

$$\frac{dN^f}{dE\gamma} = (0.73/M_{h_a})\, x^{1.5}\ \exp -7.8\, x \tag{30}$$

with $x = E\gamma/M_{h_a}$.

Gamma Ray Yields

For the $\gamma\gamma$ or the γZ final states the yield is a Dirac delta centered respectively at M_{h_a} or $M_{h_a} - M_Z^2/(4M_{h_a})$.

- We model the delta as a Gaussian centered at the corresponding energy and of width equal to (conservatively) 15% the energy of the line.
- typically 15% is achieved e.g. in HESS and therefore such value would be conservative for the CTA.

Thus, with Gaussian width $= 0.15\ M_{h_a}$:

$$(dN/dE\gamma)^{\gamma\gamma} = 2\delta(E_\gamma - M_{h_a}) = 2(2.66/M_{h_a})\exp(-22.22(x - M_{h_a})^2/M_{h_a}^2) \tag{31}$$

and similar for γZ.

Gamma Ray Flux

The predicted gamma ray flux from annihilation of DM particles is given by the expression:

$$\frac{d\Phi_\gamma}{dE_\gamma} = \frac{1}{4\pi}\left(\int_{\Delta\Omega} d\Omega \int_{l.o.s} ds \rho_\chi^2\right)\left[\frac{1}{2M_{h_a}^2}\sum_f \sigma v_{\mathrm{rel}}(h_a h_a \to f)\frac{dN^f}{dE_\gamma}\right] \tag{32}$$

The astrophysical part is well establish from astrophysical observations and it is known as the "J-factor", we will consider the Coma Berenices dwarf as a point source with constant J-factor of $\log_{10} J = 19.52$ (with J in GeV^2 cm^{-5}).

Prediction ready

This completes the theoretical prediction by the model of the differential gamma ray flux from annihilating dark matter particles.

Likelihood Profile

Coma Berenices

We choose to make our analysis based on a simulation of future observations of the dwarf spheroidal (dSph) galaxy Coma Berenices (or Coma) by the Cherenkov Telescope Array (southern hemisphere branch).

- Coma Berenices (or Coma) was discovered in 2006 by the Sloan Digital Sky Survey.
- It is a faint Milky Way satellite at a distance of 44 kpc from the Sun.
- Coma was part of a recent study of several dSphs in a DM signal search from HESS.
- We try to follow their general analysis strategy in as much as possible as the available public tools allow us.

CTA Simulation

- We simulate an observation run of Coma of 20 hours with the southern hemisphere CTA array.
- We assume a no-result experiment, in other words we assume that no significant excess of gamma rays above nominal background is found throughout the observation period.
- From this we obtain a likelihood estimate and a test statistics (TS) from the comparison of both hypothesis, the existence or non-existence of a signal from DM annihilation.
- This technique is employed in current ID experiments to construct exclusion limits from their non-observation of significant gamma ray signals above the background.

Likelihood function

- We perform a directed scan, for each probed point (set of values of the independent parameters) in the model we feed the predicted flux to the public CTA analysis tools obtaining a likelihood estimate and a TS.
- We then supplement the estimated likelihood with information regarding unitarity and collider constraints on heavy scalars as well as the comparison with the relic abundance experimental value.
- We allow for points with relic abundance predictions below the Planck experimental bound, to account for the possibility of under-abundant DM component.

Reflected background technique

Our analysis allows us to present a likelihood profile of the parameter space of the model and estimate to what extend future observations of the CTA array can probe the model.

- We perform our analysis employing the reflected background technique where the position of the telescope aim is slightly offset from the objective.

On and Off regions

The objective is defined as a circular region (the On region, green circle) centered around Coma from which the simulated observation is used to fit against the predicted flux from the model.

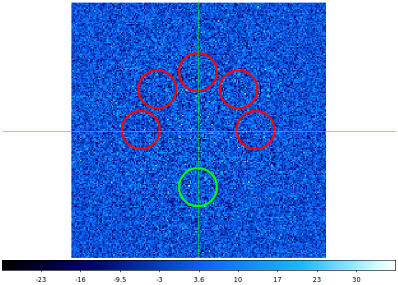

On and Off regions of the analisys

Background computation

- To compute the background several twin regions (the Off regions, red circles) are defined.
- The background rate is extracted from the public Instrument Response Function (IRF) provided by the CTA Consortium.
- The color axis is the signal detection significance (absence of notorious bright spots means that no known sources of gamma rays exist in the region).

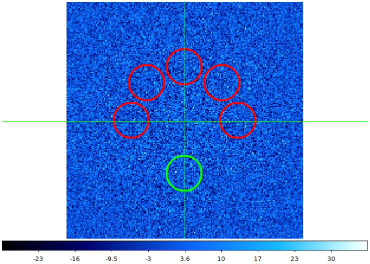

Likelihood

For the hypothesis of presence of DM, in the On/Off analysis the model M is composed of the signal (predicted number of gamma rays) and the background

$$M = M_s + M_b, \tag{33}$$

the background model M_b is taken from the background information provided in the IRF and the signal M_s is calculated from the predicted differential gamma ray flux.

Likelihood

The likelihood estimate is constructed from the formula:

$$-\log \mathcal{L}(M) = \sum_i s_i(M_s) + a_i(M_b)b_i(M_b) - n_i^{\rm on} \log[s_i(M_s) + a_i(M_b)b_i(M_b)] + b_i(M_b) - n_i^{\rm off} \log b_i(M_b) \quad (34)$$

where $n_i^{\rm on}$ ($n_i^{\rm off}$) is the number of events in bin i of the On (Off) region, $s_i(M_s)$ ($b_i(M_b)$) is the number of expected signal (background) counts in bin i of the On (Off) region and $a_i(M_b)$ is the ratio between the spatial integral over the background model in the On region and the Off region for bin i.

Test Statistics

The detection significance of the model is estimated using the Test Statistic (TS) which is defined as:

$$\mathrm{TS} = 2[\log \mathcal{L}(M_s + M_b) - \log \mathcal{L}(M_b)] \tag{35}$$

which involves the log-likelihood value obtained when fitting the model and the background together to the simulated data, and also the log-likelihood value when fitting only the background (no-DM hypothesis).

Results

Best Fit Point

We use a public parameter sampler and optimiser (Diver) to scan the parameter space. The best fit point (BFP) i.e. the coordinates that maximize the likelihood function present the following mass spectra for the scalar particles of the model:

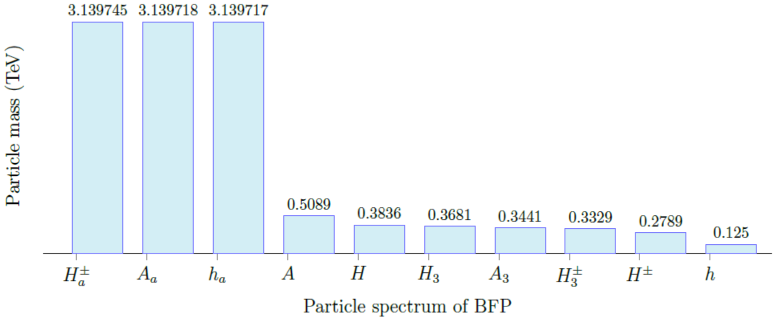

Spectrum of masses of the scalar particles at the BFP

Likelihood Profile 1

We present the normalized likelihood profile as a function of the annihilation cross section and the DM candidate mass

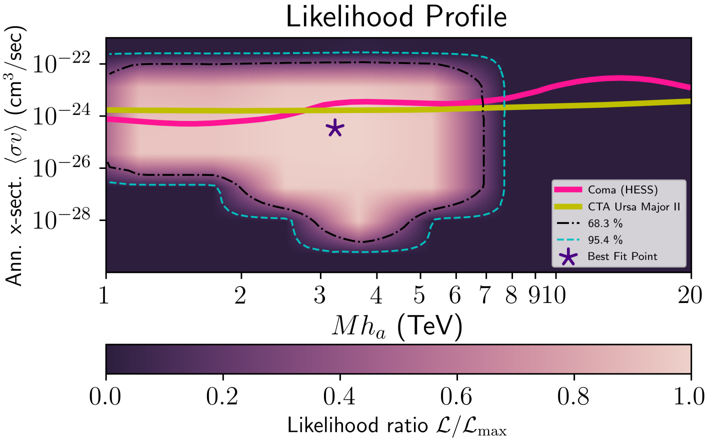

Likelihood Profile 2

The BFP of the analysis is marked with an asterix.

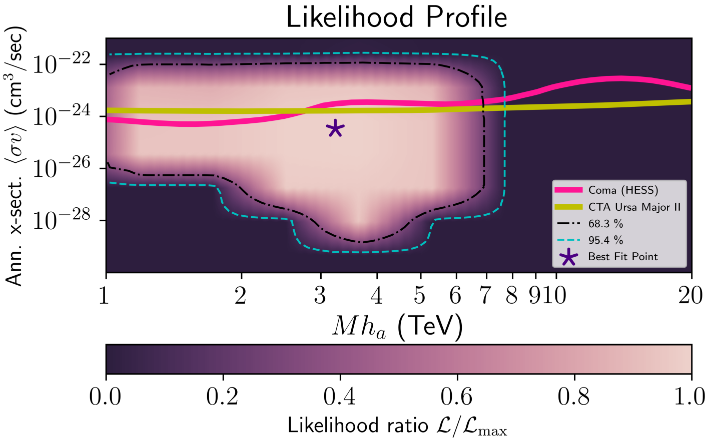

Likelihood Profile 3

Contours for a coverage probability of 68% and 95% for two degrees of freedom are shown.

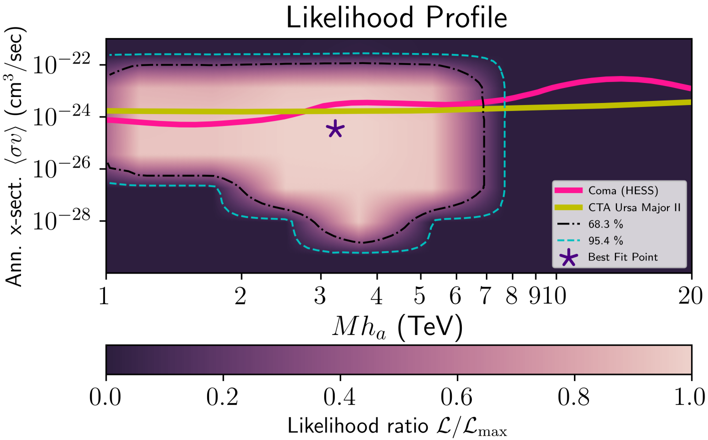

Likelihood Profile 4

We show exclusion curves from an analysis of an observation of Coma by HESS (model independent).

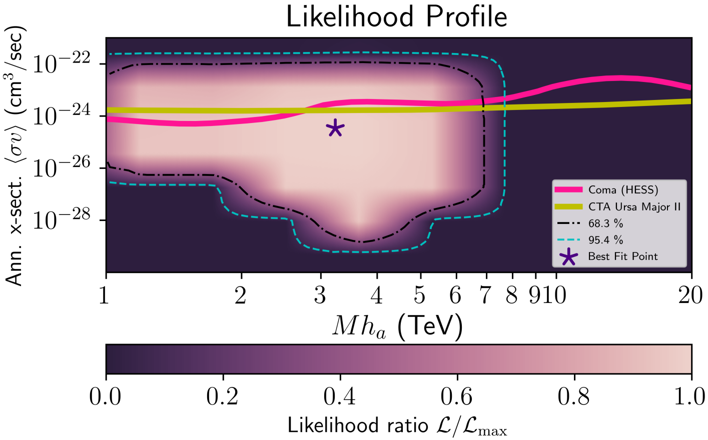

Likelihood Profile 5

And a simulation of a CTA observation of Ursa Major II (model independent).

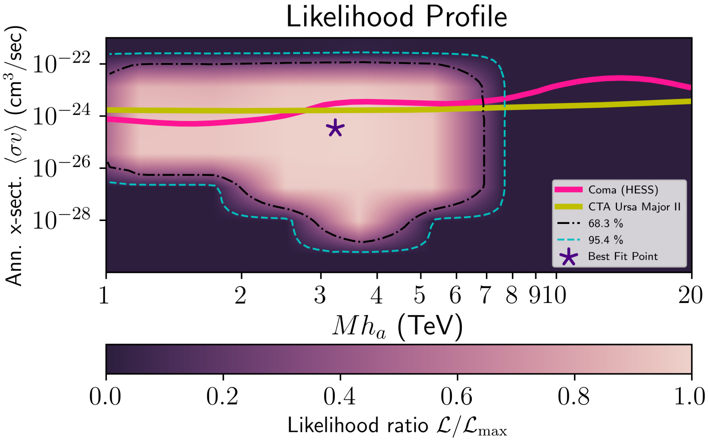

Likelihood Profile 6

Darker regions have a very small likelihood value and so are not favoured by the analysis.

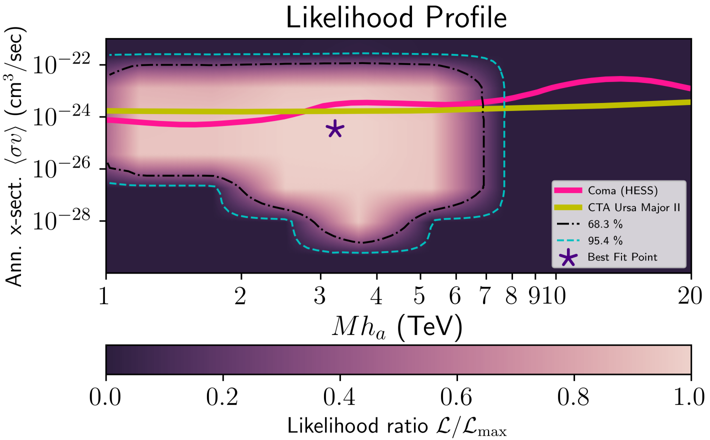

Likelihood Profile 7

Note how the region above a DM mass of 5 TeV is gradually disfavored.

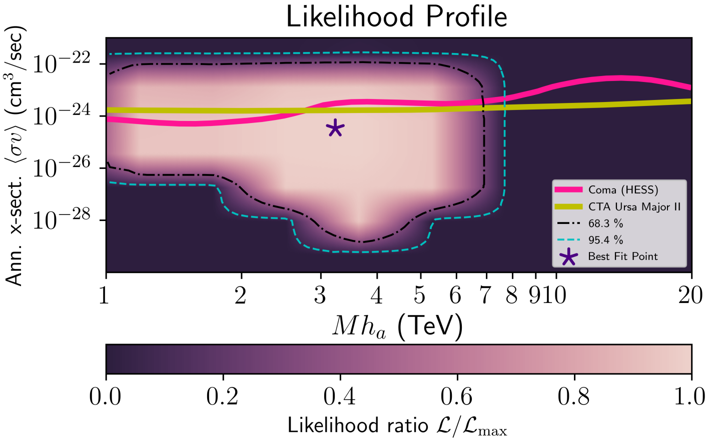

Likelihood Profile 8

Close to a third of the viable region of plausible physical points lie above the two exclusion curves.

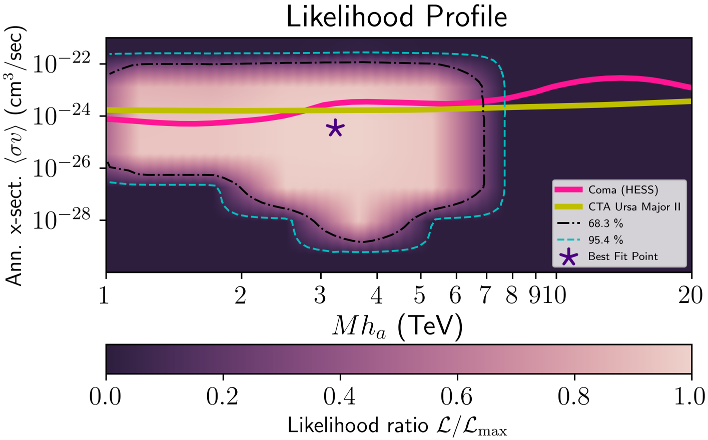

Likelihood Profile 9

Both exclusion curves come very close to disfavour the best fit point of the model.

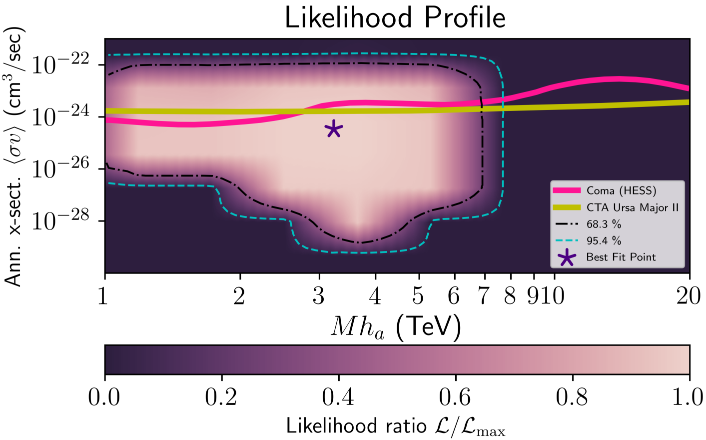

Relic Abundance 1

Scatter plot of points of the model and their predictions of the value of the relic abundance.

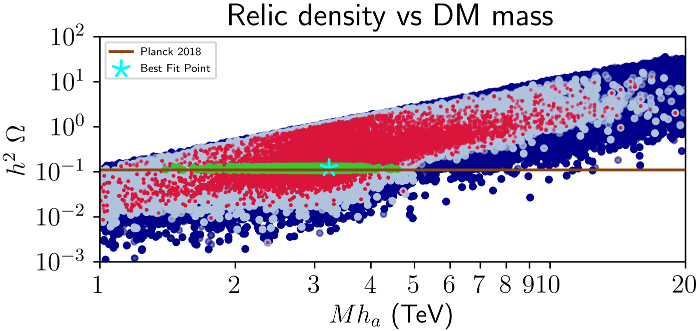

Relic Abundance 2

The points are color coded according to weather or not they satisfy all physical constraints.

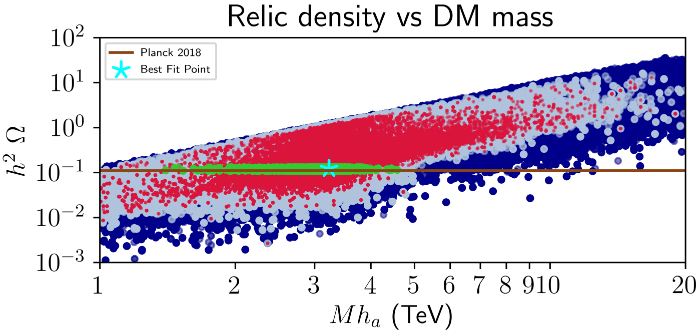

Relic Abundance 3

Navy blue points are consistent with unitarity and stability bounds but are excluded from experimental scalar searches.

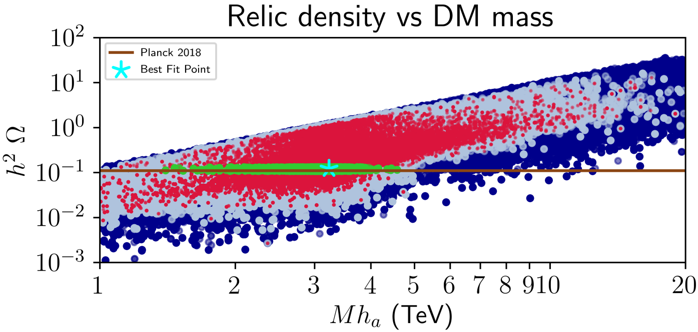

Relic Abundance 4

Light blue points are consistent with all of these constraints.

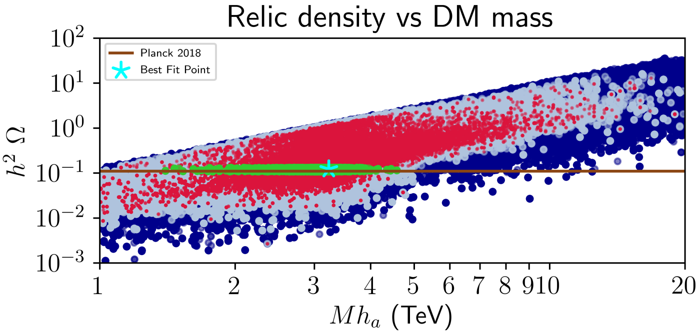

Relic Abundance 5

The red points in addition satisfy the decoupling limit for h.

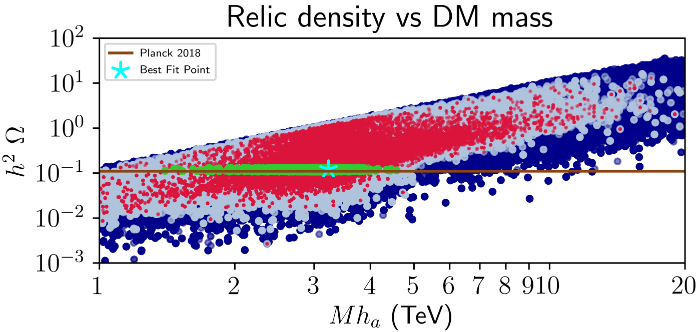

Relic Abundance 6

Green points predict a relic abundance within the experimental Planck value.

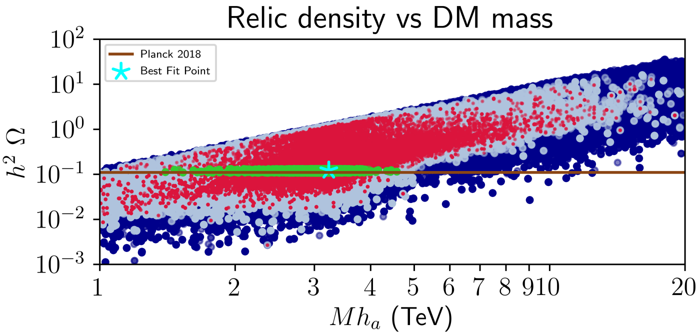

Relic Abundance 7

Almost all of the points above a DM mass of ~ 5 TeV predict overproduction of DM.

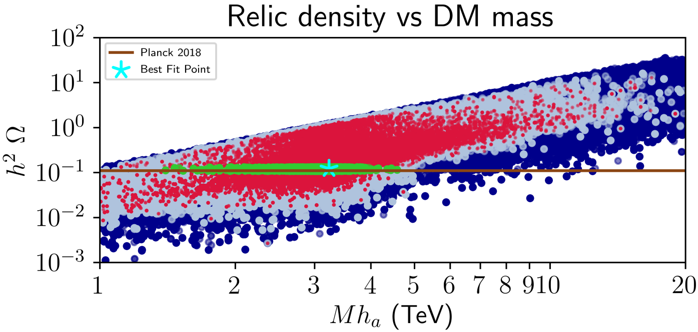

Relic Abundance 8

Which explains the fact that this region is disfavoured in the likelihood profile.

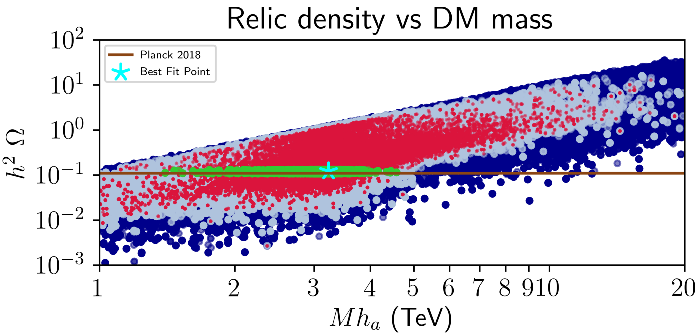

Cross Section 1

Scatter plot of the annihilation cross section as a function of the DM mass, the color code of the points is the same as before.

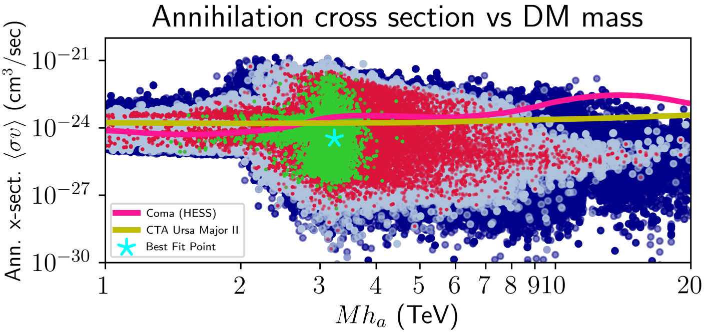

Cross Section 2

There is a "depression" starting around masses of 2 TeV where the cross section begins to take smaller values.

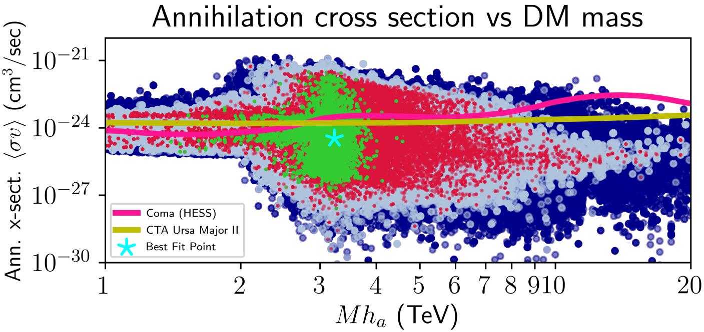

Cross Section 3

This may be indicative that the destructive interference of the enhancement factors in between 2 and 3 TeV values of the DM mass is a generic feature.

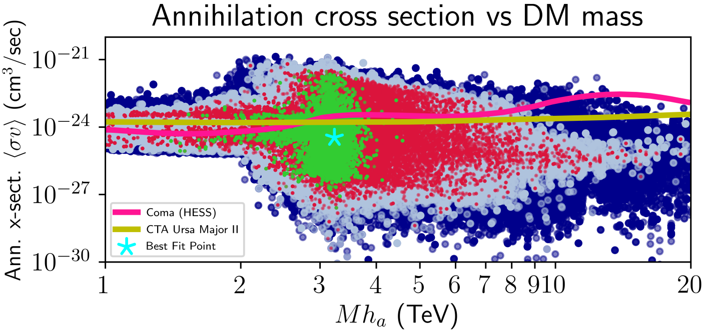

$\tan(\theta)$

Scatter plot of the DM mass as a function of $\tan\theta$, points predicting a relic abundance value within the experimental interval lie mostly between values of $\tan\theta$ equal 2 and 4, with the BFP attaining a value of 2.34.

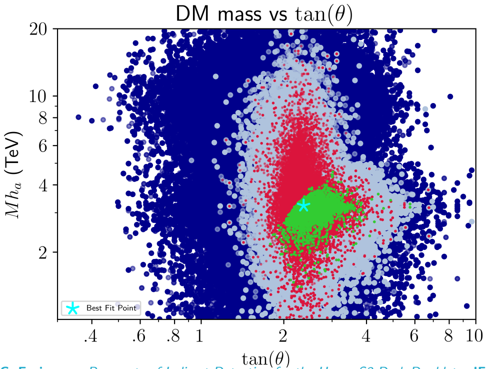

Test Statistics 1

Scatter plot of the TS as a function of the DM mass in the DM mass range between 1 and 5 TeV.

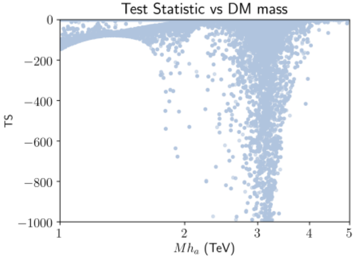

(a)

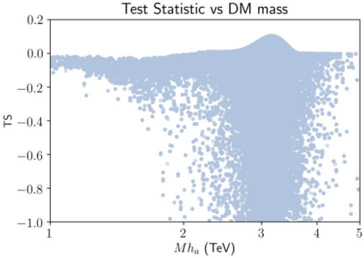

(b)

Test Statistics 2

All the points shown satisfy all constraints and lie in or below the experimental Planck value.

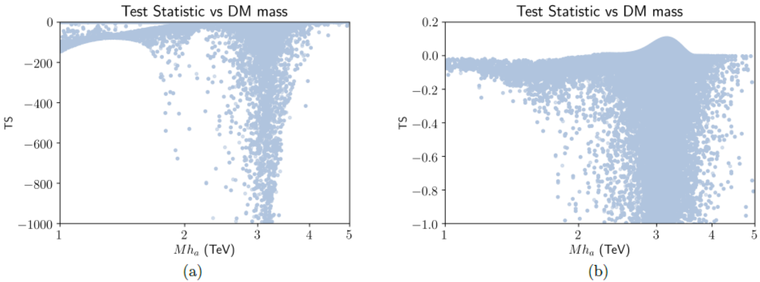

Test Statistics 3

We note that the TS reaches an almost constant maximum value very close to zero for a given mass.

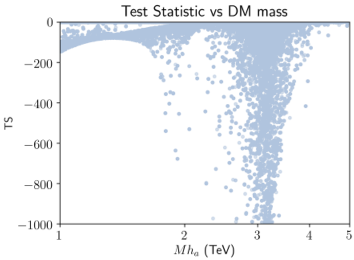

(a)

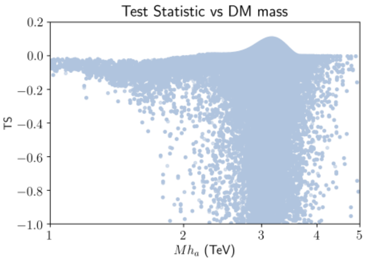

(b)

Test Statistics 4

With a small bulb around a DM mass of ∼3.2 TeV, attaining a maximum TS close to 0.1.

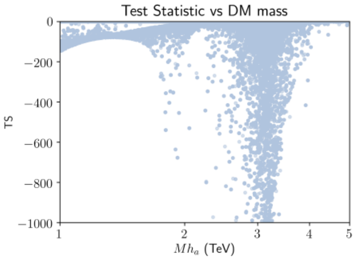

(a)

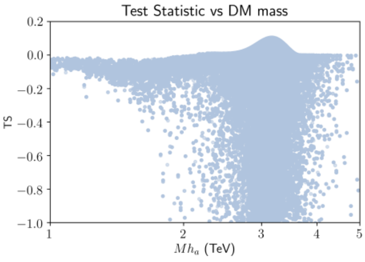

(b)

Test Statistics 5

For points in this figure lying in a (vertical) ray of constant DM mass, we consider the difference $TS_{\max} - TS \equiv \Delta TS$.

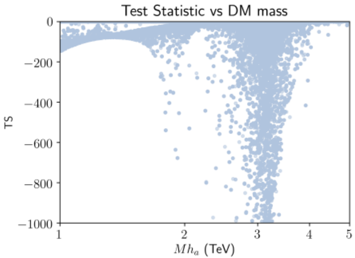

(a)

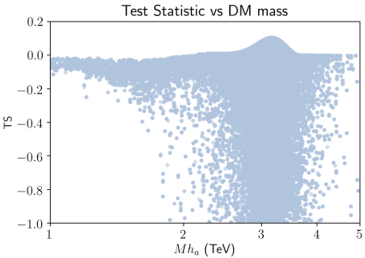

(b)

Test Statistics 6

A value of $\Delta TS = 1$ corresponds to a coverage probability of 68.3% for estimation of 1 parameter, which we take as the annihilation cross section.

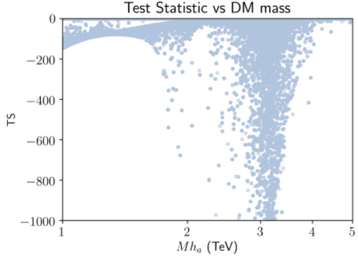

(a)

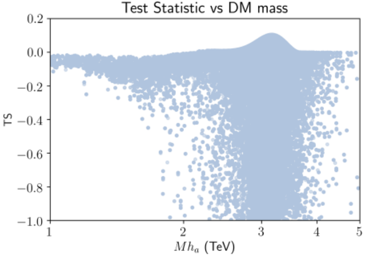

(b)

Test Statistics 7

Therefore, we interpret points in such a ray with $\Delta TS > 1$ as excluded with a C.L. of 68%.

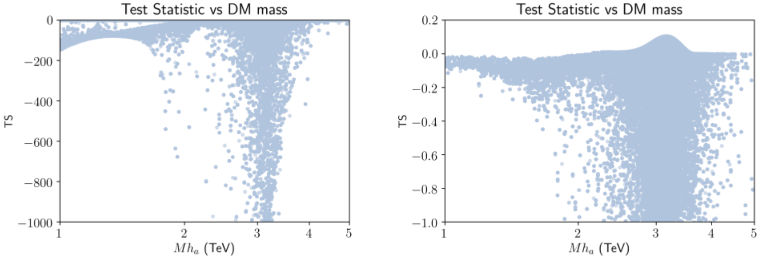

(a) (b)

Test Statistics Profile 1

In this manner we construct a "Test Statistic profile", points colored according to their value of the Test Statistic.

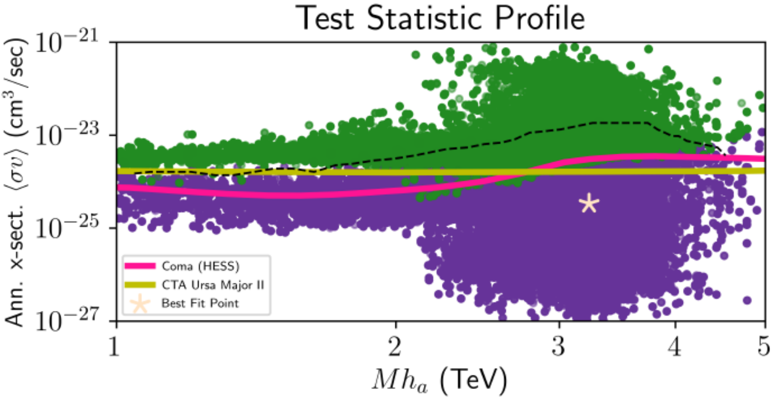

Test Statistics Profile 2

Since the value of $TS_{\max}$ is very small, for points such that $\Delta TS \gtrsim 1$ we approximate $\Delta TS \approx |TS|$ and the limit condition becomes $|TS| > 1$.

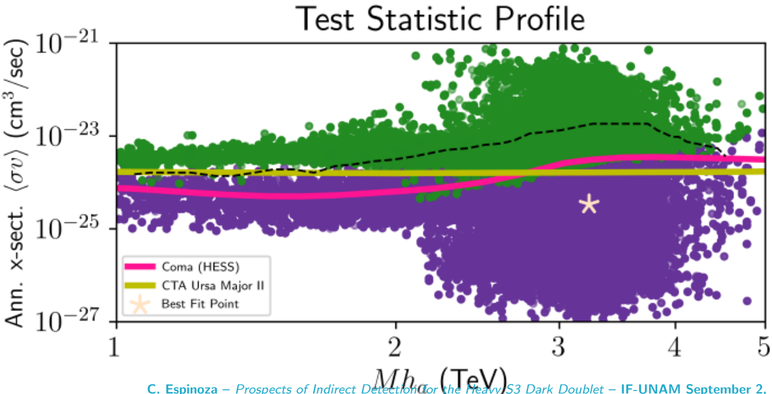

Test Statistics Profile 3

We consider the points in the upper region ($|TS| > 1$) of this figure excluded by our analysis (at a C.L. of 68%) while the points in the bottom ($|TS| < 1$) region are not.

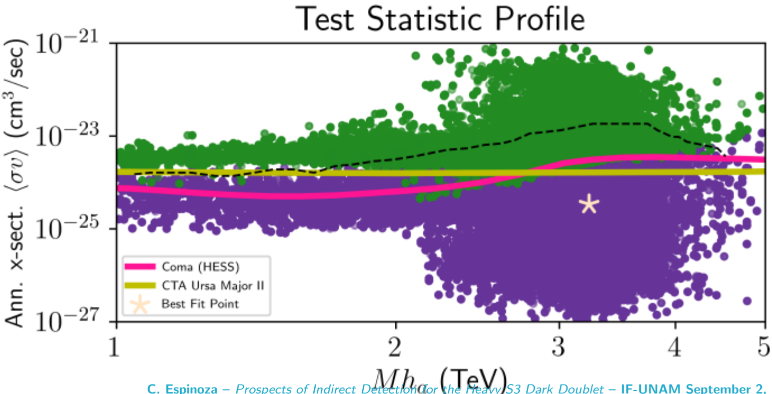

Test Statistics Profile 4

We can then interpret the boundary of the upper (green) region as an approximate exclusion curve.

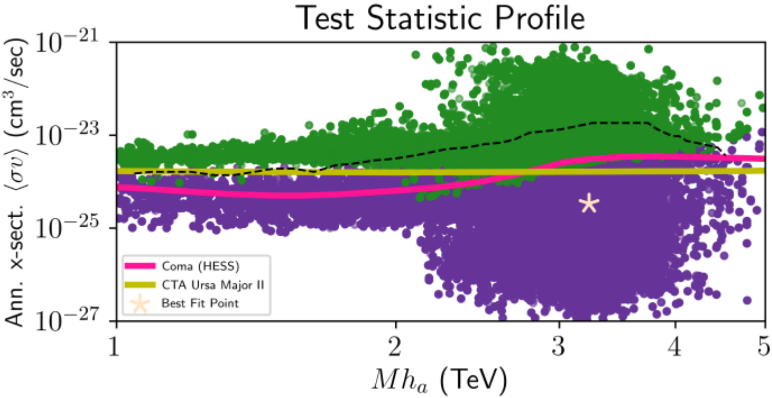

Test Statistics Profile 5

There is an overlapping of the two regions, which we take as a consequence of the error bars of the analysis.

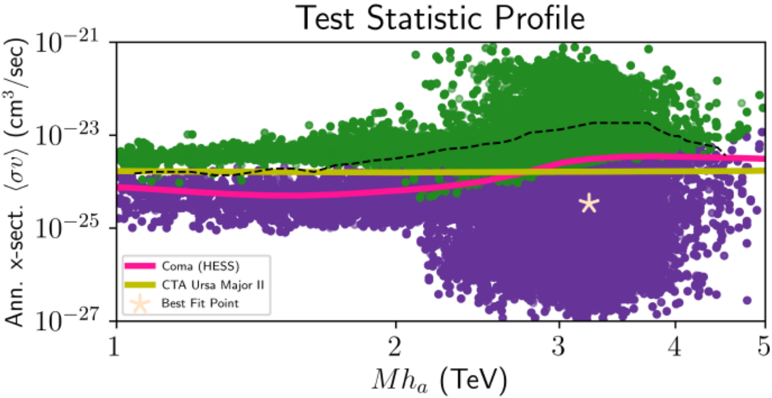

Test Statistics Profile 6

Though a precise determination of these errors will not be pursued here.

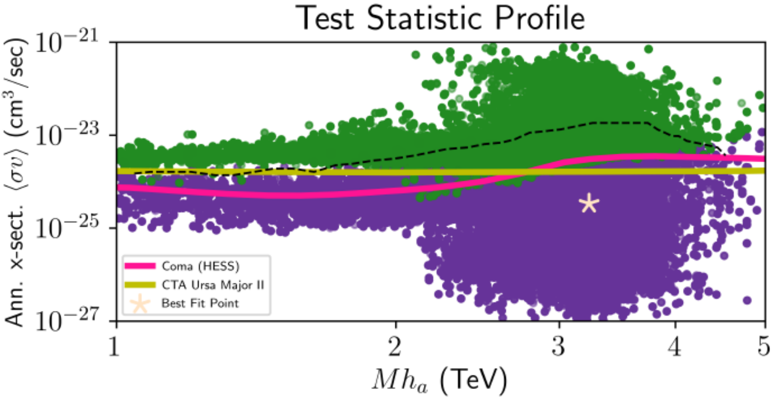

Conclusions

Conclusions 1

- We determined the likelihood profile in parameter space of the Dark S3 model from a simulation of an observation run of the Coma dwarf galaxy at the CTA.
- DM masses above 5 TeV are exclude mainly because of overproduction of DM not consistent with the observed value of the relic abundance.
- For masses below 5 TeV the best fit point of the likelihood analysis gives a DM value of $\sim$ 3.14 TeV, somewhat higher than the value where the highest cross section enhancement occurs, indicating that other constraints such as unitarity and scalar searches are also important for the precise determination of the best fit.

Conclusions 2

- Comparison of our results with independent analysis in the literature shows that current as well as estimated exclusion limits are close to disfavour the model's BFP.
- Perhaps the inclusion of a combined analysis taking into consideration several more dwarf galaxies will allow more stringent limits on the model.

Acknowledgments

Acknowledgments

We acknowledge the use of the following public tools, many thanks to their developers!

- CalcHEP - A package for calculation of Feynman diagrams and integration over multi-particle phase space.
- ctools - Cherenkov Telescope Array Science Analysis Software.
- Diver - A fast parameter sampler and optimiser based on differential evolution.
- FeynArts - A Mathematica package for the generation and visualization of Feynman diagrams and amplitudes.
- FeynCalc - Tools and Tables for Quantum Field Theory Calculations.
- FormCalc - A Mathematica package for the calculation of tree-level and one-loop Feynman diagrams.
- HiggsBounds - Testing BSM Higgs sectors against limits from LEP, Tevatron and LHC Higgs searches.
- Micromegas - A code for the calculation of Dark Matter Properties.
- Pippi - Painless parsing, post-processing and plotting of posterior and likelihood samples.
- SARAH - A Mathematica package for building and analyzing SUSY and non-SUSY models.
- Spheno - S(upersymmetric) Pheno(menology).

Acknowledgments

- This research has made use of the CTA instrument response functions (version prod3b-v2) provided by the CTA Consortium and Observatory,
- This research is partly supported by UNAM PAPIIT through Grant IN111518.
- C.E. acknowledges the support of Conacyt (México) Cátedra 341.

Thank you for your attention!